Journal of Sound and Vibration (2002) **257**(1), 89–106
doi:10.1006/jsvi.5030, available online at http://www.idealibrary.com on IDEAL®

STRATEGY FOR FINDING A NEAR-OPTIMAL MEASUREMENT SET FOR PARAMETER ESTIMATION FROM MODAL RESPONSE

T. Pothisiri and K. D. Hjelmstad

Department of Civil and Environmental Engineering, University of Illinois, Urbana, IL 61801*, USA*

(*Received* 15 *December* 2000, *and in final form* 7 *January* 2002)

Algorithms that estimate structural parameters from modal response using least-squares minimization of force or displacement residuals generally do not have unique solutions when the data are spatially sparse. The number and character of the multiple solutions depend upon the physical features of the structure and the locations of the response measurements. It has been observed that both the number of solutions and the sensitivity of the parameter estimates to measurement noise is greatly influenced by the choice of measurement locations. In this paper, we present a heuristic method to select a near-optimal subset of measurement locations starting from a particular set of measurements, by minimizing the sensitivity of the parameter estimates with respect to observed response. The statistical properties of solution clusters generated from a Monte Carlo samples of noisy data are used to determine the best candidate measurement to be dropped from the current set. The process is repeated until solution sensitivity cannot be significantly reduced. We also show that the laborious Monte Carlo computations can be avoided in certain cases by using a direct computation of sensitivity estimates. A numerical example is provided to illustrate the method and to examine the performance of the proposed algorithm.

1. INTRODUCTION

Certain parameter estimation schemes are based upon measured natural modes and frequencies of a structure [1–3]. These parameter estimation methods use a parameterized finite element model of the structure to estimate the values of the parameters using a least-squares minimization of either the force residual or displacement residual of the vibration eigenvalue problem. Generally, the accuracy of parameter estimation is affected by the number of the measured natural modes, the location of the sensors that measure the modal displacements, and the accuracy of the measurements obtained through the testing process [4]. Often the number of modes that one can measure is limited by the physical features of the structure, the method of excitation, and the absolute resolution of the sensors. The accuracy of the sensors is, of course, always a key issue and one should endeavor to use the most accurate instruments possible. However, the accuracy of the measurement is a feature of the instrument that often cannot be significantly changed after the instruments are selected and certainly cannot be changed after the measurements have been made.

Proper selection of the sensor locations is essential to ensure a successful parameter estimation in the presence of the measurement error [5]. By adjusting sensor locations one can improve the outcome of parameter estimation even if the accuracy of the measurements and the number of measurable modes is fixed. There are two opportunities

0022-460X/02/$35.00

to affect improvements within the context of sensor location. The first, and most obvious, is in the initial deployment of the instruments prior to testing. The second opportunity comes from the observation that it is not always better to have more measurement locations because errors in locations that are highly sensitive to error can pollute the parameter estimates. By using the measurements at a certain subset of model degrees of freedom (i.e., by ignoring some of the measurements), one can reduce the overall error in the parameter estimates that is caused by measurement noise.

Several heuristic methods have been proposed in the literature to select a near-optimal set of measurement locations for noise-polluted data. These methods were originally used in the context of selecting the sensor and actuator locations to control the dynamic response of the structure [6–8]. In the context of nondestructive testing of structures subjected to static excitation, Sanayei *et al.* [5] used Delorenzo's method [6] to select a subset of noisy force and displacement measurements to reduce the error in the parameter estimates. Error sensitivity analysis was used to determine the smallest subset of applied forces and measured displacements that would result in the least overall error in the identified parameters. In particular, the largest element of the error sensitivity matrix of the parameter estimation algorithm was used as an index to compare different candidate sets of measurements. The sensitivities required by the algorithm were computed by the finite difference method. This approach requires repeated evaluation of the input–output error relationship to guide the improvement of the results. The method is limited to the problem of establishing the initial instrument locations because the method does not include a means of removing information from the measurement set.

In this paper, we present an algorithm for establishing a near-optimal deployment of sensors for parameter estimation from modal response. The method is based on an observation by Hjelmstad [4] that there is an essential coupling between the multiplicity of solutions to the parameter estimation problem and the sensitivity to noise. The optimal measurement set will be the one that is least sensitive to noise because these are the most likely to cluster tightly around the noise-free solutions in simulations and are least likely to be affected by estimation bias. The non-uniqueness, which helps to tighten the noisy solution clusters, presents the obvious and important issue of sorting out which solution corresponds to the best estimates for the given problem. Selecting the best estimate at each step of the algorithm is crucial to successfully determining a near-optimal measurement set.

The search for the best measurement set is an integer programming problem. We present a heuristic method for executing this search to avoid exhaustive enumeration. This simplification substantially reduces the computation required but means that there is no guarantee that an absolute optimum will be found. We adopt the output-error least-squares estimator of Banan and Hjelmstad [9] to develop the method, but suggest that the parameter estimation step at the core of this algorithm could be done by any of a number of alternative approaches. We use a simple random-starting-point method to find the multiple minima at each parameter estimation step and identify the best solution as the one for which the value of the parameter estimation objective function associated with the mean of the parameter estimates for each Monte Carlo solution cluster is the least. The eigenvalues of the covariance matrix of the parameter estimates associated with the identified solution are used to determine which measurement location should be dropped at each level of the measurement selection process.

We propose the substitution of a sensitivity-based estimate of the solution cluster statistics that can be used in lieu of generating a Monte Carlo sample. When this is appropriate one can realize substantial computational savings. The most important feature of the proposed algorithm is that it generalizes well to problems for which

visualization of the clustering is not possible (i.e., any problem with more than two or three parameters). A numerical example is provided to illustrate the method and examine the performance of the proposed algorithm.

2. STRUCTURAL MODELLING AND PARAMETER ESTIMATION FROM MEASURED MODAL RESPONSE

Assume that the structure can be characterized by a linear finite element model with N_d degrees of freedom. Following common practice let us further assume that the mass $\mathbf{M}$ is constant and known in advance while the linear stiffness $\mathbf{K}$ of the structure is parameterized by N_p constitutive parameters $\mathbf{x}$ as

$$\mathbf{K}(\mathbf{x}) = \mathbf{K}_0 + \sum_{k=1}^{N_g} \sum_{m \in \Omega_k} f_m(x_k)\mathbf{G}_m, \tag{1}$$

where $\mathbf{K}_0$ is the part of the stiffness matrix that is known *a priori*, $f_m(x_k)$ is the (possibly non-linear) constitutive parameter function, and $\mathbf{G}_m$ is the kernel matrix for element m in the group Ω_k. The element kernel matrices essentially contain the geometrical information of the structural element, and are independent of the element constitutive parameters. Based on the parameter grouping scheme of Hjelmstad *et al.* [10], we assume that a group of elements Ω_k. can be characterized by a single stiffness parameter x_k. Further, we assume that each of the elements in the structural model is associated with one of the parameter groups $\{\Omega_1, \Omega_2, \ldots, \Omega_{N_g}\}$ where N_g is the number of different parameter groups in the model. As such, the parameter associated with element $m \in \Omega_k$ is x_k.

To fix ideas, let us summarize the parameter estimation scheme used in the present study. The output error estimator of Banan and Hjelmstad [9] is chosen for modal parameter estimation because of its ability to handle spatially sparse data sets without sacrificing computational efficiency. In addition, the output error estimator has a relatively low bias for a wide range of measurement noise.

Free undamped vibrational response of a structure gives rise to the generalized eigenvalue problem

$$\mathbf{K}(\mathbf{x})\boldsymbol{\phi}_i = \lambda_i \mathbf{M}\boldsymbol{\phi}_i \tag{2}$$

in which λ_i and $\boldsymbol{\phi}_i$ represent the eigenvalue (the square of the natural frequency) and the eigenvector (mode shape) for the ith vibration mode. We shall assume that the natural frequency and natural mode can be measured in a modal test.

Let $\hat{\aleph}_i$ be the set of degrees of freedom of the finite element model associated with measurement locations on the test structure for mode i and let $\bar{\aleph}_i$ be the set of remaining (unmeasured) degrees of freedom for that mode. The number of degrees of freedom that are measured is denoted as $\hat{N}_d^i$ and the number of degrees of freedom that are not measured is denoted as $\bar{N}_d^i$. We can reorder and partition the eigenvector as

$$\tilde{\boldsymbol{\phi}}_i \equiv \mathbf{P}_i\tilde{\boldsymbol{\phi}}_i = \begin{bmatrix} \hat{\boldsymbol{\phi}}_i \\ \bar{\boldsymbol{\phi}}_i \end{bmatrix}. \tag{3}$$

where $\mathbf{P}_i$ is a column-wise permutation of the identity matrix, $\hat{\boldsymbol{\phi}}_i$ and $\bar{\boldsymbol{\phi}}_i$ are the submatrices of the eigenvector components associated with the measured and unmeasured degrees of freedom, respectively, for mode i. In accord with the above permutation, the structural system matrices can also be redefined as

$$\tilde{\mathbf{K}}_i \equiv \mathbf{P}_i\mathbf{K}\mathbf{P}_i^{\mathrm{T}}, \quad \tilde{\mathbf{M}}_i \equiv \mathbf{P}_i\mathbf{M}\mathbf{P}_i^{\mathrm{T}}. \tag{4}$$

Let $\tilde{\mathbf{M}}_i = [\hat{\mathbf{M}}_i | \bar{\mathbf{M}}_i]$ be a partitioning of the mass matrix into a part $\hat{\mathbf{M}}_i$ associated with the measured degrees of freedom $\hat{\aleph}_i$, and a part $\bar{\mathbf{M}}_i$ associated with unmeasured degrees of freedom $\bar{\aleph}_i$. We define the matrix $\mathbf{B}_i(\mathbf{x})$ as

$$\mathbf{B}_i(\mathbf{x}) \equiv \tilde{\mathbf{K}}_i(\mathbf{x}) - \lambda_i [\mathbf{O}_i | \bar{\mathbf{M}}_i], \tag{5}$$

where $\mathbf{O}_i$ is an $N_d \times \hat{N}_d^i$ zero matrix. With these definitions we can rewrite equation (2) in the equivalent form

$$\mathbf{B}_i(\mathbf{x}) \tilde{\boldsymbol{\phi}}_i = \lambda_i \hat{\mathbf{M}}_i \hat{\boldsymbol{\phi}}_i. \tag{6}$$

The right-hand side of the above equation involves only the measured response $\hat{\boldsymbol{\phi}}_i$ rather than a complete response vector. Let $\mathbf{Q}_i$ be the $\hat{N}_d^i \times N_d$ boolean matrix that extracts the components of the response vector associated with measured degrees of freedom from the reordered eigenvector by the relationship $\hat{\boldsymbol{\phi}}_i = \mathbf{Q}_i \tilde{\boldsymbol{\phi}}_i$. Premultiplying equation (6) by $\mathbf{B}_i^{-1}(\mathbf{x})$ and operating with $\mathbf{Q}_i$ results in a convenient measure of error for the output error estimator [9]

$$\mathbf{e}_i(\mathbf{x}) \equiv \hat{\boldsymbol{\phi}}_i - \lambda_i \mathbf{Q}_i \mathbf{B}_i^{-1}(\mathbf{x}) \hat{\mathbf{M}}_i \hat{\boldsymbol{\phi}}_i. \tag{7}$$

The output error estimator can now be cast as the least-squares optimization problem

$$\underset{\mathbf{x} \in \mathscr{R}^{N_p}}{\text{Minimize}} \quad J(\mathbf{x}) \equiv \frac{1}{2} \sum_{i=1}^{N_m} \delta_i ||\mathbf{e}_i(\mathbf{x})||^2, \tag{8}$$

where δ_i is the weight factor for the ith mode and $N_m \ll N_d$ is the number of modes with measured natural frequencies and mode shapes. The weight factor δ_i is assigned *a priori* to reflect the relative confidence in the data for each mode and to establish an appropriate scaling of the measurements. This optimization problem is often solved as a constrained minimization with bounding values on the parameters. For the above parameter estimation problem, an index of identifiability can be defined as $\beta \equiv N_m \hat{N}_d / N_p$. This index is simply the ratio of available data to the unknowns. If $\beta < 1$, the parameter estimates will be unreliable. On the other hand, reliable parameter estimation is possible if $\beta \geqslant 1$. The constrained least-squares problem (8) can be solved using a recursive quadratic programming algorithm. The computations can be based on the Gauss–Newton approximation of the Hessian of the objective to avoid computing second derivatives of the error function $\mathbf{e}_i(\mathbf{x})$. The implementation of the algorithm is described in detail by Banan and Hjelmstad [9]. Note that for the present application the measurement locations are taken to be the same for all modes. Hence, $\hat{\aleph}_i = \hat{\aleph}$, $\bar{\aleph}_i = \bar{\aleph}$, $\hat{N}_d^i = \hat{N}_d$, and $\bar{N}_d^i = \bar{N}_d$ in the sequel.

3. NON-UNIQUENESS OF MODAL PARAMETER ESTIMATION

Structural parameter estimation algorithms from measured modal response generally do not have unique solutions when the data are spatially sparse [4]. The extra solutions are local extrema of the parameter estimation objective function and are generally extraneous. In the literature, only a few articles have been devoted to the question of uniqueness of solution in the structural parameter estimation problem. Some of the proposed parameter estimation algorithms implicitly avoid the problem of non-uniqueness by finding the solution nearest to a set of nominal model parameters. Such methods assume that the desired parameters are close to the nominal parameters and that there are no spurious solutions in the neighborhood of the correct solution. These assumptions are not tenable for some parameter estimation problems, such as in the problem of damage detection,

where the nominal values of the parameter estimates of the structural model are not known in advance. One approach to the non-uniqueness problem is to use a random starting point scheme in conjunction with the objective minimization algorithm to find all of the multiple minima of the parameter estimation problem [4]. With a sufficiently large sample of starting points, one can assess the multiplicity of solutions with confidence.

Hjelmstad [4] observed that for noise-free simulated measurements the correct solution can generally be distinguished from the extraneous solutions by a considerably larger and deeper basin of attraction, which is indicated both by a larger fraction of solutions attracted from the random starting points and by a lower average value of the objective function. The situation is more complicated for noise-polluted data, where parameter estimates are scattered due to noise. The identified multiple solutions exhibit different levels of sensitivity to random noise for different patterns of measurement. Further, the sensitivity of the parameter estimates to noise in the data depends upon the number and density of solutions to the parameter estimation problem. Nevertheless, the study showed that there is a clear connection between multiple solutions associated with noise-free data and the distinct clusters of results with noisy data. Because solution multiplicity is so important to the proposed algorithm we shall describe the random starting point method in a bit more detail.

The solution of the parameter estimation problem described by equation (8) depends upon the topography of the objective function $J(\mathbf{x})$. When the measured data are spatially sparse, the objective function is usually non-linear and multiple minima are possible. Each local minimum represents a candidate solution to the parameter estimation problem. The final outcome of the iterative parameter estimation process depends on the initial guess of parameters $\mathbf{x}^0$ that must be specified to start the iteration. Each starting point converges to the minimum within its basin of attraction (that is the definition of the basin of attraction). The situation is illustrated in Figure 1 for a three-dimensional parameter space. In this illustration, we assume that there are two solutions, $\mathbf{x}_A$ and $\mathbf{x}_B$. From the seven starting points $\{\mathbf{x}_1^0, \mathbf{x}_2^0, \ldots, \mathbf{x}_7^0\}$, five of them converge to one or the other of the two solutions while starting points $\mathbf{x}_2^0$ and $\mathbf{x}_5^0$ get bound at the constraints $x_3 = 0$ and $x_2 = x_2^U$, respectively. In the illustration the area inside the dashed rectangular parallelepiped represents a feasible domain of the parameter estimates determined by the lower bounds $\{x_1^L, x_2^L, x_3^L\}$ and the upper bounds $\{x_1^U, x_2^U, x_3^U\}$, respectively. These bounds must be selected properly in order

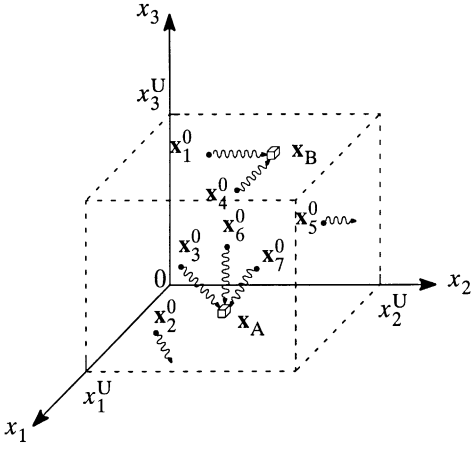

Figure 1. The result of parameter estimation from different starting points.

for the parameter estimates to make any physical sense. Often, parameter values can be set to zero as natural lower bounds. The upper bounds, however, must be selected so that they provide a sufficiently large domain for possible solutions to the parameter estimation problem.

Since it is impossible to know in advance the number of solutions for equation (8) and their distribution, we adopt the random starting point scheme proposed by Hjelmstad [4] wherein a sample of N_r random starting points $\{\mathbf{x}_1^0, \mathbf{x}_2^0, \ldots, \mathbf{x}_{N_r}^0\}$ is used to seed the search for solutions. Each of these starting points that converges will find a solution to the parameter estimation problem. The collection of these solutions is a subset of the complete solution set. To assess the multiplicity of solutions with confidence, one must use a sufficiently large sample of starting points.

In this study, we assume prior knowledge of the baseline structural model. Hence, we can select our random starting points from within a bounded region centered at the point associated with the baseline parameter values, $\mathbf{x}^*$. To avoid starting from points that are likely to get stuck at bounding constraints, the ith starting point is chosen to lie within a hyper-ellipsoid centered at $\mathbf{x}^*$. Let $\mathbf{x}_j^0$ denote the ith starting point in the N_p-dimensional parameter space. The ith starting point is allowed into the sample only if

$$(\mathbf{x}_i^0 - \mathbf{x}*)^{\mathrm{T}}\mathbf{A}(\mathbf{x}_i^0 - \mathbf{x}*) \leqslant 1, \tag{9}$$

where $\mathbf{A}$ denotes a scaling matrix, which is defined as $\mathbf{A} \equiv \mathrm{diag}[1/x_1^{*2}, 1/x_2^{*2}, \ldots 1/x_{N_p}^{*2}]$. The idea of restricting the starting parameter values is shown schematically for a three-dimensional parameter space in Figure 2 where x_1^*, x_2^*, and x_3^* are the three components of the solution point associated with the baseline parameters. In the figure, the area inside the rectangular parallelepiped bounded at $\{x_1^U, x_2^U, x_3^U\}$ represents the feasible domain of the parameter estimates. The random starting points can be easily generated one component at a time using a random number generator and then accepted or rejected according to equation (9).

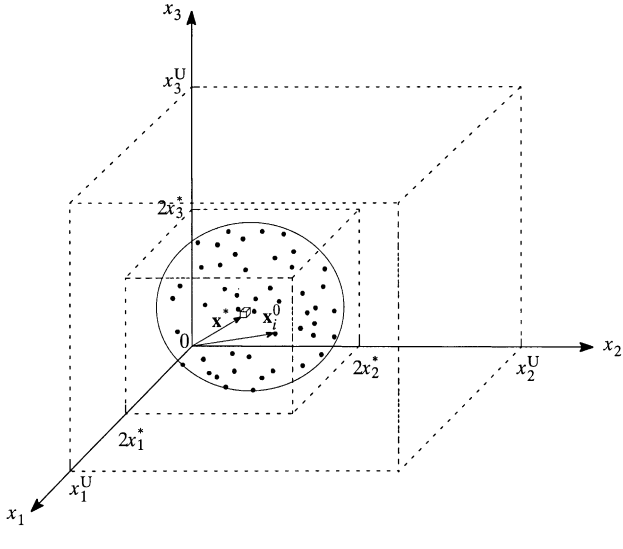

Figure 2. The schematic representation of the simulated random starting points.

4. MEASUREMENT ERROR SENSITIVITY ANALYSIS OF MULTIPLE SOLUTIONS

The multiplicity of solutions in modal parameter estimation is further complicated by the presence of noise in the measured data. Typically, different sets of noisy measurements will yield different outcomes of parameter estimation due to the effect of noise on the topography of the objective function $J(\mathbf{x})$. To account for the sensitivity of system parameters due to noise, Shin and Hjelmstad [11] adopted a data perturbation scheme to generate a Monte Carlo sample of parameter estimates by adding a random perturbation with known statistical properties to the measured data. Let the jth component of the perturbed eigenvector be calculated from the jth component of the ith measured eigenvector as

$$\tilde{\boldsymbol{\phi}}_{ij} = \hat{\boldsymbol{\phi}}_{ij}(1 + a\eta_{ij}), \tag{10}$$

where η_{ij} is a uniform random variate in the range $[-1, 1]$ and a is the noise amplitude. This model represents band–limited white noise, but can easily be modified to include colored noise. The data perturbation scheme can be used to obtain the sensitivity information for each of the (noise-free) multiple solutions identified from the random starting point scheme by using the individual solution as a fixed starting point for each perturbed data set. Since each perturbation iteration requires one execution of the parameter estimation algorithm, the Monte Carlo approach can be computationally intensive as the number of perturbation iterations becomes large.

In the Monte Carlo method, once a sample of solution points has been created using the random-starting-point and the data-perturbation schemes, the correct solution must be identified from the available solutions in the sample. In general, each of these solution points will be clustered in the vicinities of the noise-free solutions as shown in Figure 3 for a three-dimensional parameter space. In this figure we assume that four solution points $\{\mathbf{x}_A, \mathbf{x}_B, \mathbf{x}_C, \mathbf{x}_D\}$ have been identified from random starting points. The groups of solutions essentially represent clustering of local minima of the perturbed objective functions. The distribution of the solution points within each cluster location indicates the sensitivity of a local minimum of the objective function $J(\mathbf{x})$ due to the random perturbation. As such, each individual cluster can be regarded as a set of perturbed solutions to the parameter estimation problem.

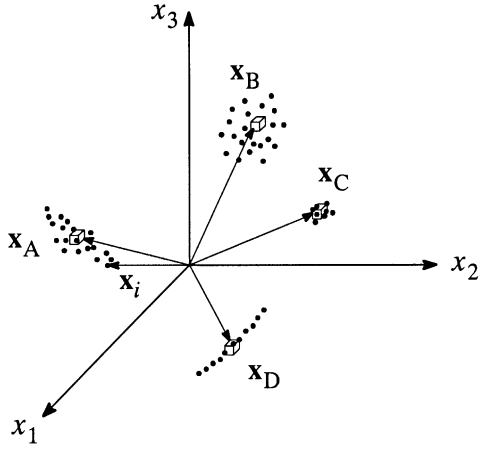

Figure 3. Noisy solution points in three-dimensional parameter space.

In general the cluster of solutions associated with the correct solution can be distinguished from the extraneous ones by a considerably larger and deeper basin of attraction. The latter condition is indicated by a lower averaged objective function. A precise set of parameter estimates is the one that is insensitive to noise and is indicated by compactness of the cluster. For a simple structural model with two or three parameters, the measure of compactness can be obtained directly from the plot of the solution points on a three-dimensional parameter space. However, this is not the case for an N_p-parameter model where such a plot is not feasible. As such, a mathematical description of a cluster is required.

One can use the statistical properties of the solutions inside a cluster to identify its shape. For example, the mean and standard deviation can be used to measure bias and spread of the solutions due to the data perturbation respectively. However, as illustrated in Figure 4 for a two-parameter case, the standard deviation may not provide sufficient information to identify the correct shape of a cluster. On the other hand, the eigenvalues of the covariance matrix of the estimated parameters provide a more accurate basis for estimating the appearance of a cluster. The covariance matrix of parameters for cluster can be estimated as

$$\mathbf{R}^{\mathbf{x}} = \frac{1}{N}\sum_{i=1}^{N} \mathbf{x}_i \otimes \mathbf{x}_i - \frac{1}{N}\sum_{i=1}^{N} \mathbf{x}_i \otimes \frac{1}{N}\sum_{i=1}^{N} \mathbf{x}_i, \tag{11}$$

where N is the number of solutions belonging to the cluster and $\otimes$ indicates the tensor product. In general, the parameter estimates are accurate if the eigenvalues of the covariance matrix are small.

As previously mentioned, the Monte Carlo method is computationally expensive because the non-linear optimization process is repeated many times. Alternatively, one can obtain the sensitivity of parameter estimates to random perturbation by using the optimum sensitivity approach of Araki and Hjelmstad [12]. In this method, the mean and covariance of the system parameters are estimated using the optimum sensitivity derivatives, which can be computed by direct differentiation of the Kuhn–Tucker optimality criterion. As such, the method is computationally efficient compared with the Monte Carlo approach. In addition, this approach is generally more efficient than the finite difference approach used by Sanayei *et al.* [5], and does not require the assessment of numerical errors. However, the optimum sensitivity method can be unreliable when the system output-system parameters relation is highly non-linear, in which case the Monte Carlo method is more robust (as discussed in reference [12]). In the current study, we

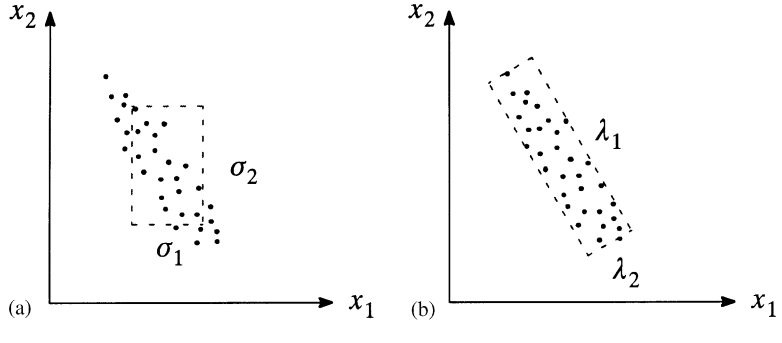

Figure 4. Two different statistical description of a cluster. (a) σ_i, standard deviations; (b) λ_i, eigenvalues of covariance.

implement the optimum sensitivity method to determine the sensitivity of the parameter estimation solutions with respect to the data perturbation scheme, as described below.

For the sake of the present development let us define a measurement vector $\hat{\mathbf{\Phi}}$ to be the concatenation of the measurements from each measured mode of mode shapes as $\hat{\mathbf{\Phi}}^{\mathrm{T}} \equiv \{\hat{\boldsymbol{\phi}}_1^{\mathrm{T}}, \hat{\boldsymbol{\phi}}_2^{\mathrm{T}}, \ldots, \hat{\boldsymbol{\phi}}_{N_n}^{\mathrm{T}}\}$. Let $\hat{\mathbf{\Phi}}$ denote the kth component of $\hat{\mathbf{\Phi}}$ and note that the range of the index is $k = 1,2,\ldots,N_m\hat{N}_d$. For the perturbation method [11, 12] we introduce a perturbed vector of the measured mode shapes $\tilde{\mathbf{\Phi}}$ that have the following mean and covariance relationship with the measured values:

$$\hat{\mathbf{\Phi}} = E[\tilde{\mathbf{\Phi}}], \qquad R^{\mathbf{\Phi}} = E[(\tilde{\mathbf{\Phi}} - \hat{\mathbf{\Phi}}) \otimes (\tilde{\mathbf{\Phi}} - \hat{\mathbf{\Phi}})], \tag{12, 13}$$

These properties are established from the properties of the random noise that is superimposed on the measured values to create the perturbed values. For a certain solution $\mathbf{x}$ that has been determined using the random starting point algorithm, we can estimate the mean $\bar{\mathbf{x}}$ and covariance $\mathbf{R}^{\mathbf{x}}$ of parameter estimates due to the measurement perturbation using the following approximation [12]:

$$\bar{\mathbf{x}} \equiv E[\mathbf{x}(\tilde{\mathbf{\Phi}})] \approx \mathbf{x}(\hat{\mathbf{\Phi}}) + \frac{1}{2}\sum_{k=1}^{N_m\hat{N}_d}\sum_{i=1}^{N_m\hat{N}_d} \mathbf{x}_{,ki}\,(\hat{\mathbf{\Phi}}) R^{\mathbf{\Phi}}_{ki}, \tag{14}$$

$$\begin{aligned}\mathbf{R}^{\mathbf{x}} &\equiv E[(\mathbf{x}(\tilde{\mathbf{\Phi}}) - \bar{\mathbf{x}}(\tilde{\mathbf{\Phi}})) \otimes (\mathbf{x}(\tilde{\mathbf{\Phi}}) - \bar{\mathbf{x}}(\tilde{\mathbf{\Phi}}))] \\ &\approx \sum_{k=1}^{N_m\hat{N}_d}\sum_{l=1}^{N_m\hat{N}_d} \mathbf{x}_{,k}\,(\hat{\mathbf{\Phi}}) \otimes x_{,l}\,(\hat{\mathbf{\Phi}}) R^{\mathbf{\Phi}}_{kl}.\end{aligned} \tag{15}$$

In the above equations, the first and second order optimum sensitivity derivatives are indicated by $\mathbf{x}_{,k} \equiv \partial\mathbf{x}/\partial\hat{\mathbf{\Phi}}_k$ and $\mathbf{x}_{,kl} \equiv \partial^2\mathbf{x}/\partial\hat{\mathbf{\Phi}}_i\partial\hat{\mathbf{\Phi}}_l$ respectively. As shown by Araki and Hjelmstad [12] these derivatives can be obtained simply by solving systems of linear equations (one for each) involving the gradients of the error function $\mathbf{e}_i(\mathbf{x})$ defined in equation (7). Complete details of this computation as well as comparisons with the Monte Carlo approach are described in reference [12]. If the perturbed measurements are created by imposing uniform random noise of amplitude a, in accord with equation (10), equations (14) and (15) simplify to

$$\bar{\mathbf{x}}(a) = \mathbf{x}(\hat{\mathbf{\Phi}}) + \frac{a^2}{6}\sum_{k=1}^{N_m\hat{N}_d} \mathbf{x}_{,kk}\,(\hat{\mathbf{\Phi}})\hat{\mathbf{\Phi}}_k^2, \tag{16}$$

$$\mathbf{R}^{\mathbf{x}}(a) = \frac{a^2}{3}\sum_{k=1}^{N_m\hat{N}_d}\sum_{l=1}^{N_m\hat{N}_d} \mathbf{x}_{,k}\,(\hat{\mathbf{\Phi}}) \otimes \mathbf{x}_{,l}\,(\hat{\mathbf{\Phi}})\hat{\mathbf{\Phi}}_k\hat{\mathbf{\Phi}}_l. \tag{17}$$

This noise model is used throughout the remainder of this paper.

The mean and covariance of the parameter estimates can be computed for each of the candidate solutions identified from the random starting point scheme. In this manner we can evaluate the nature of the clustering of noisy solutions for each candidate solution. In the present application we need to identify the best solution from among the several candidates for each measurement set and from those best candidates select the one least sensitive to noise. The correct solution $\mathbf{x}^{**}$ can be obtained as the set of parameters $\bar{\mathbf{x}}$ associated with the global minimum $J(\bar{\mathbf{x}})$. Note that the identification of this best solution is different for the Monte Carlo approach as opposed to the statistical estimates (which is simply given as the estimate computed from the measured data). In the Monte Carlo approach the mean of the estimates is generally not equal to the estimate from the measured data.

5. SELECTION OF MEASUREMENT LOCATIONS FOR ERROR REDUCTION

In this section, we describe a heuristic method that makes use of the error sensitivity analysis of the previous section to select a near-optimal subset of the initial measurement locations. The method takes into account the possibility of solution multiplicity of the modal parameter estimation problem. Unlike the finite difference approach of Sanayei *et al*. [15], Monte Carlo simulations are not required to establish the input–output error relationships of the identified parameters in the present method. It should be noted that the identified subset of measurement locations is not guaranteed to minimize the error in the parameter estimates. Selection of the optimal subset of measurements would require an exhaustive search of the different combinations of the measured degrees of freedoms The exact solution of the integer programming problem is prohibitive. The present method is intended to guide the selection of a near-optimal subset of the measurement locations for a relatively modest computational effort. While this algorithm will seldom find the actual optimum it will almost always lead to an improved solution.

Let us suppose that an initial set of measurement locations $\hat{\mathbf{\Phi}}_0$ is given as known information. One can find the global optimum $\mathbf{x}^{**}(\hat{\mathbf{\Phi}}_0)$ corresponding to $\hat{\mathbf{\Phi}}_0$, as described in the previous section. The eigenvalues of the covariance matrix of parameter estimates $\mathbf{R}^{\mathbf{x}^{**}}$, evaluated from equation (17), quantify the sensitivity of $\mathbf{x}^{**}$ to the random perturbations. As mentioned earlier, the estimated parameters are expected to be accurate when these eigenvalues are small. In the current algorithm, we use the value of the objective function and the eigenvalues of the covariance matrix associated with the global minimum to measure the accuracy and the sensitivity of the parameter estimation results respectively. In particular, we propose a search scheme to find a set of measurement locations that minimizes $J(\mathbf{x}^{**})$ and the sum of the squares of the eigenvalues of $\mathbf{R}^{\mathbf{x}^{**}}$.

The selection of a near-optimal subset of measurement locations can be described as an integer programming process as illustrated in Figure 5. In the illustration, the (global parameter estimation) (GPE) algorithm indicates the process of finding the global minimum of the parameter estimation objective function using the random starting point

1. Initialization
   1.*a*. Set $i = 0$, $\hat{\mathbf{\Phi}}_i = \hat{\mathbf{\Phi}}_0$ is given data.
   1.*b*. Compute $\mathbf{x}_0^{\bullet\bullet}$ by *GPE* algorithm.
   1.*c*. Compute $J_0 = J(\mathbf{x}_0^{\bullet\bullet}, \hat{\mathbf{\Phi}}_0)$, $\mathbf{R}_0 = \mathbf{R}^{\mathbf{x}_0^{\bullet\bullet}}(\hat{\mathbf{\Phi}}_0)$, $s_0 = \sum_{i=1}^{N_p} \lambda_i^2(\mathbf{R}_0)$.
   1.*d*. Set $n_0 = \hat{N}_d$, $J_0^{\min} = J_0$, $s_0^{\min} = s_0$

2. Measurement selection process
   2.*a*. If insufficient data remains, **EXIT**.
   2.*b*. Do $j = 1,\ldots, n_i$
      2.*b.i*. Create $\hat{\mathbf{\Phi}}_i^{(j)}$ by dropping the jth entry in $\hat{\mathbf{\Phi}}_i$ for all modes.
      2.*b.ii*. Solve for $\mathbf{x}_j^{\bullet\bullet}$ by *GPE* algorithm.
      2.*b.iii*. Compute $J_i^{(j)} = J(\mathbf{x}_j^{\bullet\bullet}, \hat{\mathbf{\Phi}}_i^{(j)})$, $\mathbf{R}_i^{(j)} = \mathbf{R}^{\mathbf{x}_j^{\bullet\bullet}}(\hat{\mathbf{\Phi}}_i^{(j)})$, $s_i^{(j)} = \sum_{i=1}^{N_p} \lambda_i^2(\mathbf{R}_i^{(j)})$.
      2.*b.iv*. If $J_i^{(j)} < J_i^{\min}$ and $s_i^{(j)} < s_i^{\min}$ then $j_i^{\min} = j$.
   2.*c*. Set $\hat{\mathbf{\Phi}}_{i+1} \leftarrow \hat{\mathbf{\Phi}}_i^{(j_i^{\min})}$, $J_{i+1}^{\min} = J_i^{(j_i^{\min})}$, $s_{i+1}^{\min} = s_i^{(j_i^{\min})}$.
   2.*d*. Test for termination.
      If $J_{i+1}^{\min} \geq J_i^{\min}$ or $s_{i+1}^{\min} \geq s_i^{\min}$ then **EXIT**
   2.*e*. Set $i \leftarrow i + 1$, $n_i \leftarrow n_i - 1$.
   2.*f*. Go to 2.*a*.

Figure 5. Algorithm for selection of a near-optimal subset of measurement locations.

scheme along with the associated perturbation sensitivity analysis. Let the sum of the squares of the covariance matrix of parameters $\mathbf{x}$ be defined as

$$s \equiv \sum_{i=1}^{N_p} \lambda_i^2(\mathbf{R}^{\mathbf{x}}). \tag{18}$$

When a measurement location is dropped, the mode shape information at the dropped location is disregarded for all measured modes.

The proposed algorithm provides explicit information on the sensitivity of parameter estimates (as well as the objective function) to the level of measurement noise for each of the measurement patterns investigated. The value of the objective function is used to guarantee the improvement in the values of the parameter estimates. There is no significant computational burden associated with recomputing the objective function for a selected subset of measurements. When the system output–system parameter relationship is highly nonlinear (e.g., when the level of uncertainty in the measurement is great or when the measured data are very sparse) the Monte Carlo approach to the sensitivity analysis will give better results.

In practice, the proposed strategy for finding the near-optimal set of measurement locations can be used either in a pretest simulation study prior to a non-destructive testing or to reduce error of the parameter estimation results for a given data set. The starting point for the pretest study might be a complete measurement set but would probably work best by starting from an assortment of different feasible measurement sets. The various solutions can then be evaluated to account for unmodeled phenomena.

6. A NUMERICAL EXAMPLE

In this section, we examine the performance of the present algorithm through a simulation study. The example structure is the six-story shear building with fixed base shown in Figure 6. The structural model has six degrees of freedom, the horizontal translations at the story levels, all of which are included in the initial measurement set. The structure is parameterized with six parameters, $\mathbf{x} = \{x_1, x_2, \ldots, x_6\}^{\mathrm{T}}$. The stiffness of the ith

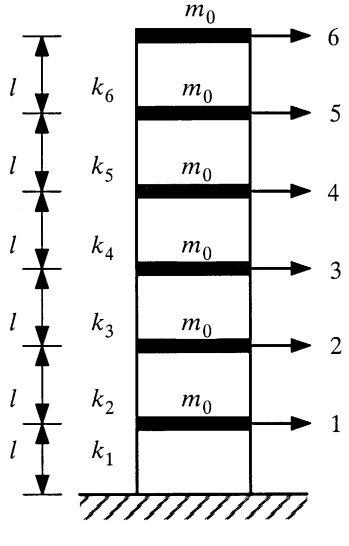

Figure 6. The six-degree-of-freedom shear building.

story is given by $k_i = x_i k_0$. The nominal properties of the structure are chosen such that $k_0/m_0 = 1{\cdot}2\,\mathrm{s}^2$. Let us assume that the actual parameters associated with the current conditions of the structure are $\mathbf{x} = \{2{\cdot}0,\ 2{\cdot}0,\ 2{\cdot}0,\ 1{\cdot}0,\ 1{\cdot}0,\ 1{\cdot}0\}^{\mathrm{T}}$. Note that the prior knowledge of the actual values of parameters is not required in the current algorithm. Within the simulation context these values can be used to judge the outcome of the parameter estimation algorithm. In the current study, we assume that the baseline parameters associated with the initial structure are given as $\mathbf{x}^* = \{3{\cdot}0,\ 3{\cdot}0,\ 2{\cdot}0,\ 2{\cdot}0,\ 1{\cdot}0,\ 1{\cdot}0\}^{\mathrm{T}}$. The specified values of baseline parameters are used in the random starting point scheme to identify the multiple solutions to the parameter estimation problem for each pattern of measurements investigated. These values can be selected to be different from the above set without significantly changing the results of the simulation study. The current sets of parameters reflect a damage scenario in which x_1 and x_2 have decreased by 33% and x_4 has decreased by 50%.

The results from a free vibration analysis of the current structural model are shown in Table 1 where the ith mode shape $\boldsymbol{\psi}_i$ is computed from $\mathbf{K}(\hat{\mathbf{x}})\boldsymbol{\psi}_i = \lambda_i \mathbf{M}\boldsymbol{\psi}_i$ and is scaled such that $\boldsymbol{\psi}_i^{\mathrm{T}}\mathbf{M}\boldsymbol{\psi}_i^{\mathrm{T}} = 1$. The denomination of "level" refers to story level, as defined in Figure 6. The natural frequencies and mode shapes of all six mode, as listed in this table, are taken as our nominal initial data. We generate simulated "measured data" by adding random noise with known statistical properties to the noise-free data. The kth component of the lth noisy measurement vector from the kth component of the computed noise-free measurement vector is

$$\hat{\phi}_{kl} = \psi_{kl}(1 + \varepsilon\zeta_{kl}), \tag{19}$$

where ζ_{kl} is a uniform random variate in the range $[-1, 1]$. The amplitude ε will be used in our study to quantify the level of noise in the measurement. Throughout the study we will assume that the natural frequencies can be measured with negligible error and are considered to be noise-free.

During the measurement selection process in the algorithm, different patterns of measurements are used as input to the parameter estimation problem. Each case that we examine will be designated by the degrees of freedom which are measured. For example, the measurement case 12–4–6 uses modal displacements at levels 1, 2, 4 and 6 and does not use measurements at levels 3 and 5. In all measurement cases, all of the six available modes will be used.

In the current simulation study, we generate 100 noisy data sets based upon the noise-free data from Table 1 in accord with equation (19) using three levels of noise: $\varepsilon = 5$, 10 and

TABLE 1

Noise-free data from free vibrational analysis of the current structure

	First mode	Second mode	Third mode	Fourth mode	Fifth mode	Sixth mode
Natural frequency (Hz)	0·05350	0·14050	0·22465	0·30364	0·43324	0·45008
Mode shape						
Level 1	0·03263	−0·09481	−0·10439	0·12439	−0·18499	−0·17133
Level 2	0·06373	−0·15884	−0·12212	0·06013	−0·00938	−0·22824
Level 3	0·09183	−0·17129	−0·03847	−0·09533	0·18452	−0·13273
Level 4	0·13937	−0·08495	−0·19270	−0·11710	−0·14704	−0·02988
Level 5	0·17380	0·05656	0·10393	0·21631	0·09464	−0·00666
Level 6	0·19186	0·16133	−0·15740	−0·10639	−0·03265	0·00118

20% respectively. Each of the simulated noisy data sets are used as input as the initial measurements from which the algorithm is performed to selectively eliminate the measured degrees of freedom until the near-optimal set of measurement locations is obtained. The measurement subset to which the algorithm will converge depends upon the specific features of the data that drives the algorithm. Therefore, it is interesting to see how the algorithm responds to different incarnations of noise. We make this assessment by determining the outcome of applying the algorithm for each of the 100 different incarnations of noisy data.

For each noisy measurement case to which the algorithm is applied we use 100 random starting points to identify multiple solutions to the parameter estimation problem. Hence, each column of Table 2 represents 10 000 minimizations (100 random starting points times 100 noisy measurements) of the objective function $J(\mathbf{x})$ of equation (8). The global minimum $\mathbf{x}^{**}$ for each data set is located as described previously. We compute the mean and the covariance matrix of the parameter estimates associated with the global minimum in accord with equations (16) and (17) respectively. Note that the amplitude of perturbation a in these equations is selected as the same as the level of noise ε present in the measured data. In the present simulations, we assume the a priori knowledge of the level of uncertainty in the measurement. Thus, the amplitudes of perturbation can be selected as $a = 0{\cdot}05$, $0{\cdot}10$ and $0{\cdot}20$ to characterize the bias and scatter of parameter estimates for the 5, 10 and 20% noisy measurement cases respectively.

TABLE 2

Fraction of 100 *noisy data sets converging to different patteerns of measurements for* 5, 10, *and* 20% *level of measurement noise*

	5% noise			10% nose			20% noise	
Case number	Measured d.o.f.s	Fraction	Case number	Measured d.o.f.s	Fraction	Case number	Measured d.o.f.s	Fraction
1	123–56	0·14	1	1————	0·22	1	1————	0.19
2	1—————	0·14	2	123–56	0·15	2	123–56	0·17
3	––3–––	0·11	3	––3–––	0·09	3	––3–––	0·14
4	–23–5–	0·07	4	12––5–	0·08	4	–23–5–	0·12
5	–2————	0·07	5	–23–5–	0·08	5	12————	0·07
6	–––4–6	0·06	6	–2————	0·05	6	–2————	0·06
7	12––5–	0·05	7	–––4–6	0·04	7	12–4––	0·04
8	––34–6	0·05	8	12————	0·04	8	1–345–	0·03
9	1–34–6	0·04	9	–––4––	0·04	9	–––4––	0·03
10	12————	0·04	10	12–45–	0·03	10	––34–6	0·02
11	1––4–6	0·03	11	–234–6	0·03	11	–––4––	0·02
12	12–4––	0·03	12	12–4––	0·03	12	––3–5–	0·02
13	–––4––	0·03	13	––––5–	0·02	13	––––5–	0·02
14	123–5–	0·02	14	1234––	0·01	14	123–5–	0·02
15	12–45–	0·02	15	123–5–	0·01	15	123–5–	0·01
16	1–345–	0·02	16	1–345–	0·01	16	1–34–6	0·01
17	1––45–	0·02	17	1–34–6	0·01	17	–234–6	0·01
18	1––4––	0·02	18	–2345–	0·01	18	–––4–6	0·01
19	12–4–6	0·01	19	–23–56	0·01	19	12————	0·01
20	1–3–56	0·01	20	1–3––6	0·01	20	1————6	0·01
21	–234–6	0·01	21	––34–6	0·01			
22	–2–45–	0·01	22	––3–5–	0·01			
			23	–––4–6	0·01			

Several measures of identification error are used to compare the parameter estimation results of the initial and the identified patterns of measurements. We compute the average of $\mathbf{x}^{**}$ for a specified pattern of measurements based upon a certain subset of the simulated noisy database as

$$\bar{\mathbf{x}}^{**} = \frac{1}{N_t} \sum_{t=1}^{N_t} \mathbf{x}_t^{**}, \tag{20}$$

where $\mathbf{x}_t^{**}$ denotes the parameter estimates associated with the global minimum for the tth noisy measurements of the N_t simulated data sets under consideration. With the definition of $\bar{\mathbf{x}}^{**}$, the average root quadratic bias (RQB) can be defined as

$$RQB = \frac{||\bar{\mathbf{x}}^{**} - \hat{\mathbf{x}}||}{N_p ||\hat{\mathbf{x}}||} \tag{21}$$

in which $\hat{\mathbf{x}}$ are the actual parameters for the current structural model and N_p is the number of estimated parameters in the model. The quadratic bias is a measure of the distance between the expected value of the estimates $\bar{\mathbf{x}}^{**}$ and the actual parameters $\hat{\mathbf{x}}$. To measure the scatter of the parameter estimates with respect to the actual parameters, we use the average root mean square error (RMS), which is given by

$$RMS = \frac{1}{N_p ||\hat{\mathbf{x}}||} \sqrt{\frac{1}{N_t} \sum_{t=1}^{N_p} ||\mathbf{x}_t^{**} - \hat{\mathbf{x}}||^2}. \tag{22}$$

Notice that both RQB and RMS are normalized with respect to the norm of the actual parameters.

The results of an error sensitivity analysis for the case of complete measurements (123456) are shown in Figure 7. In the figure, the values of the mean of stiffness parameters obtained from equation (16) are plotted with respect to 100 noisy data sets for different levels of measurement noise. It should be noted that the solution to the parameter estimation problem for the case of complete measurements is unique for each particular noisy data set and, hence, the multiplicity of solution is not an issue. Observe that many of the parameter estimates are quite far from the actual values, that there is a tendency for the parameter estimation algorithm to overestimate, and that the variation of the parameter estimates increases with the level of noise in the measurements. The case with 20% noise level shows the greatest scatter and bias of the parameter estimation results. The complete-measurements case will be used as a basis of comparison in the sequel.

The measurement subsets identified as near-optimal by the algorithm using randomly generated data sets are shown in Table 2. The table reports the outcome of applying the algorithm to 100 noisy data sets generated for each different level of noise. Each of the 100 runs of the algorithm identifies a near-optimal measurement set. Table 2 indicates the fraction of the 100 trials that each of the various measurement subsets was identified as the best one. For example, the measurement case 123-56 was identified as best for 14 of the 100 noisy data sets for the 5% noise level. As such, this set was the most frequently identified by the algorithm as the best deployment of instruments for the given data. The table ranks the measurement subsets according to the fraction of times each was identified as best.

Let us examine in more detail the pattern of measurements 1----- with 10% noise. Table 2 indicates that this pattern was identified as best from 22% of the data sets. Figure 8 shows the evolution of the algorithm for several of the data sets. In this figure, we plot the sum of the squares of the eigenvalues of the covariance matrix for parameter estimates associated with different sequences of measurement locations during the

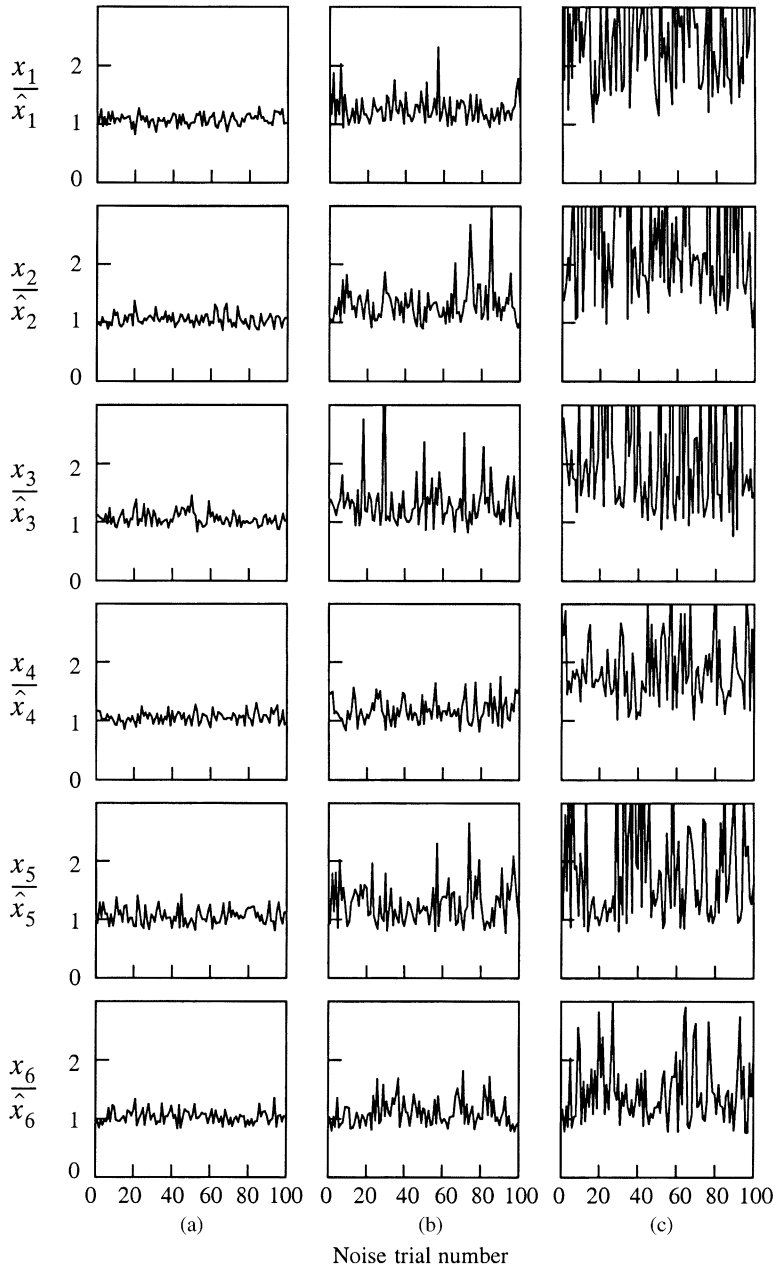

Figure 7. Variation of the mean of parameter estimates with respect to different noisy data sets using complete measurements with three levels of noise (a) 5% noise, (b) 10% noise, and (c) 20% noise.

elimination process. In the figure, λ_i denotes the ith eigenvalue of the covariance matrix. One can see that the sum of the squares of the eigenvalues decreases during the measurement selection process for each of the simulated noise trials. The reduction of the eigenvalues of the covariance matrix indicates that the outcome of the parameter estimation problem corresponding to the identified measurement locations are less sensitive to noise.

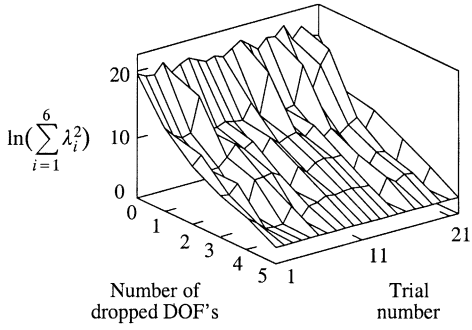

Figure 8. Sensitivity of the parameter estimates during the measurement selection process for each noisy data set with 10% level of noise that converged to the measurement case 1----- .

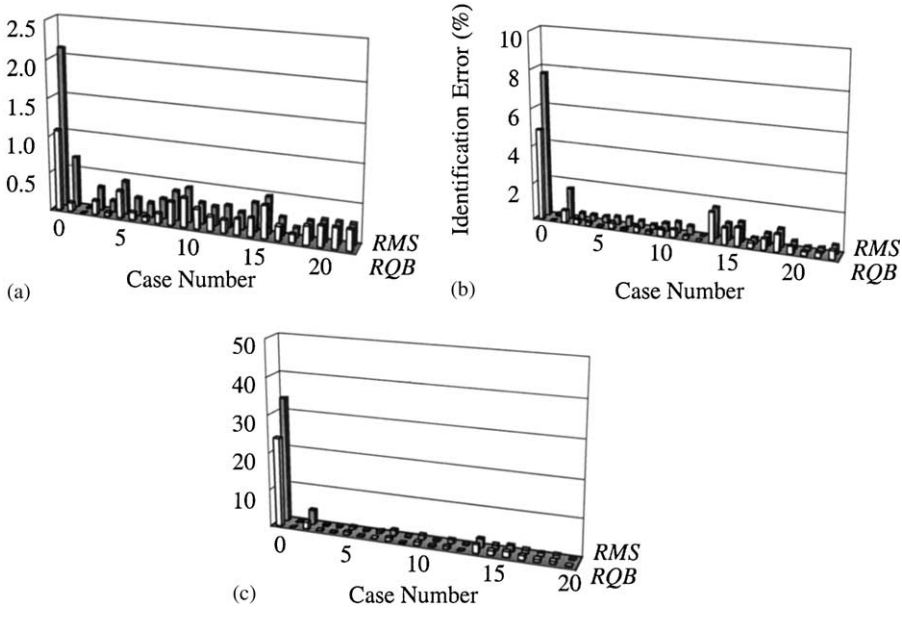

Figure 9. The identification errors of the parameter estimates for the complete–measurement case (Case 0) and the identified subsets of measurement locations from Table 2 using three different levels of noise: (a) $\varepsilon = 5\%$; (b) $\varepsilon = 10\%$; (c) $\varepsilon = 20\%$.

The identification errors of the parameter estimation results as defined by equations (21) and (22) for the complete measurement case and the identified subsets of measurement locations from Table 2 are illustrated in Figure 9. In the illustration, case 0 denotes the complete measurement case. The average (*RQB*) and the average (*RMS*) are calculated based on the noisy data sets that converged to each particular measurement case. One can observe that all measurement cases reported in Table 2 perform well for all levels of noise as indicated by the lower values of *RMS* and *RQB* compared to the complete-measurement case. The measurement case 1----- shows the least identification error for all levels of noise. Nevertheless, there is a tendency for different noisy data sets to converge to

different subsets of measured locations. A fixed subset of degrees of freedom will not be optimal for all cases of noisy measurements.

7. CONCLUSIONS

The success of a parameter estimation method depends on the behavior of the algorithm in the presence of measurement errors. One can often reduce the error in the parameter estimation by neglecting certain information. We have presented a general framework based on error sensitivity analysis to obtain a near-optimal subset of measured degrees of freedom that improve the parameter estimation results. The method is based upon the observation that there is a tradeoff between sensitivity to noise and multiplicity of solutions to the parameter estimation problem. A measurement set with more spatial sparsity will generally have more candidate minima associated with the least-squares minimization problem. Often those solutions are less sensitive to noise, as evidenced by tighter clustering of Monte Carlo samples of estimates generated from a fixed noise model. On the other hand, some deployments of instruments are intrinsically bad because they miss important features of the response.

The purpose of the algorithm proposed here is to capitalize on the observation about noise sensitivity, thereby substantially reducing concerns about bias in the non-linear least-squares estimator. There are three primary challenges: (1) identifying the best solution from among the multiple solutions, (2) efficiently estimating the sensitivity of the estimates to noise, and (3) devising a strategy for automatically identifying the best measurement set. We have employed the method of random starting points to locate the (multiple) solutions to the parameter estimation problem and identify the best solution as the one with the deepest basin of attraction. We show how the mean and covariance of estimates, needed to drive the selection algorithm, can be generated by the Monte Carlo method. We also suggest that this step can be made much more efficient using the direct sensitivity computations proposed by Araki and Hjelmstad [12]. The Monte Carlo method can be used to verify the sensitivity estimates and should replace these estimates for highly non-linear cases. With a single set of noisy data, the algorithm will search for a near-optimal subset of measurement locations that yields an improved set of parameter estimates with lower sensitivities to the measurement noise.

We have illustrated through a simple example that the data perturbation scheme and the optimum sensitivity analysis can be used to select noisy subsets of measurement locations that will produce small errors in the parameter estimates. The algorithm performed well in the illustrated example for a wide range of noise. Although we have not considered the effect of modal sparsity on the parameter estimates in the current study, one can easily imagine an extension of the proposed algorithm in which the measurement locations are not treated equally for all modes. The complexity of the search algorithm would increase, but other new possibilities (e.g., elimination of entire modes) would emerge.

REFERENCES

1. P. Hajela and F. J. Soeiro 1990 *Structural Optimization* **2**, 1–10. Recent developments in damage detection based on system identification methods.
2. K. D. Hjelmstad, M. R. Banan and M. R. Banan 1995 *Earthquake Engineering and Structural Dynamics* **24**, 53–67. On building finite element models of structures from modal response.
3. K. D. Hjelmstad and S. Shin 1996 *Journal of Sound and Vibration* **198**, 527–545. Crack identification in a cantilever beam from modal response.

4. K. D. Hjelmstad 1996 *Journal of Sound and Vibration* **192**, 581–598. On the uniqueness of modal parameter estimation.
5. M. Sanayei, O. Onipede and S. R. Babu 1992 *American Institute of Aeronautics and Astronautics Journal* **30**, 2299–2309. Selection of noisy measurement locations for error reduction in static parameter identification.
6. R. E. Skelton and M. L. Delorenzo 1983 *Journal of Large Scale Systems, Theory and Applications* **4**, 109–136. Selection of noisy actuators and sensors in linear stochastic systems.
7. R. T. Haftka and H. M. Adelman 1985 *Computers and Structures* **20**, 575–582. Selection of actuator locations for static shape control of large space structures by heuristic integer programming.
8. D. C. Kammer 1991 *Journal of Guidance, Control, and Dynamics*, **14**, 251–259. Sensor placement for on–orbit modal identification and correlation of large space structures.
9. M. R. Banan and K. D. Hjelmstad 1993 *Structural Research Series Report No. 579, UILU-ENG-93-2002, Department of Civil Engineering, University of Illinois at Urbana–Champaign*. Identification of structural systems from measured response.
10. S. Shin and K. D. Hjelmstad 1994 *Structural Research Series Report No.* 593, *UILU-ENG*-94-2013, *Department of Civil Engineering, University of Illinois at Urbana–Champaign*. Damage detection and assessment of structural systems from measured response.
11. W. K. Liu, T. Belytschko and A. Mani 1986 *Computer Methods in Applied Mechanics and Engineering* **56**, 61–81. Probabilistic finite element for nonlinear structural dynamics.
12. Y. Araki and K. D. Hjelmstad 2001 *American Institute of Aeronautics and Astronautics Journal* **39**, 1166–1174. Optimum sensitivity based statistical parameter estimation from modal response.
13. C. Papadimitriou, J. L. Beck and L. S. Katafygiotis 1997 *Journal of Engineering Mechanics, American Society of Civil Engineers* **123**, 1219–1229. Asymptotic expansions for reliability and moments of uncertain systems.
14. K. D. Hjelmstad, S. L. Wood and S. J. Clark 1990 *Structural Research Series Report No.* 557, *UILU-ENG*-90-2015, *Department of Civil Engineering, University of Illinois at Urbana–Champaign*. Parameter estimation in complex linear structures.